ACS SENSORS

pubs.acs.org/acssensors

Article

Sodium-Polyacrylate-Based Electrochemical Sensors for Highly Sensitive Detection of Gaseous Phenol at Room Temperature

Tea Romih, Eva Menart, Vasko Jovanovski, Andrej Jerič, Samo Andrenšek, and Samo B. Hočevar*

Cite This: *ACS Sens.* 2020, 5, 2570−2577

Read Online

ACCESS | Metrics & More | Article Recommendations

ABSTRACT: The detection of volatile organic compounds with electrochemical gas sensors is still very challenging regarding their sensitivity, selectivity, and operation at room temperature. There is a need for robust, sensitive, inexpensive, and yet easy-to-operate sensors for phenol and other phenolic compounds that function reliably under ambient conditions. Herein, we present a phenol gas sensor based on a combination of a semisolid, alkaline sodium polyacrylate, and commercial screen-printed electrodes. Sodium polyacrylate was employed as a multifunctional sensing material serving as a (i) gel-like electrolyte, (ii) accumulation milieu, and (iii) derivatization medium. Under ambient conditions, the sensor showed excellent sensitivity in the low ppbv (μg m^{-3}) range, a good linear operation in the examined concentration range of 0.1−1.0 ppmv for up to 105 min accumulation, and low sensitivity toward examined interferences. The sensor also indicated a possibility to differentiate between several phenolic compounds based on their oxidation potential. Given its favorable electroanalytical performance, a strong application potential is envisioned in topical fields such as environmental monitoring, cultural heritage preservation, and occupational health and safety.

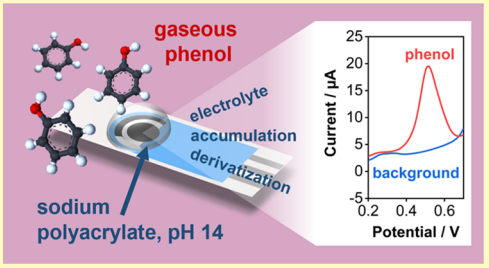

KEYWORDS: *electrochemical gas sensor, phenol, phenolic compounds, ambient conditions, cultural heritage preservation, occupational health and safety*

Phenol is a volatile organic compound listed by the European Chemicals Agency on the Priority List 1 under the REACH Regulation[1] and by the United States Environmental Protection Agency on the List of Hazardous Air Pollutants under the Clean Air Act.[2] It is known to be acutely and chronically toxic if inhaled, swallowed, or when it comes in contact with skin and eyes. It is also suspected to be mutagenic.[1] Furthermore, phenol is a degradation product of phenolic additives (stabilizers) in plastic and rubber cultural heritage objects and thus an early indicator of their deterioration in museum collections.[3] These reasons necessitate the development of reliable, sensitive, and portable phenol sensors capable of on-site detection in real time or near-real time, particularly in the fields associated with the environment, occupational health and safety, and cultural heritage preservation.

Phenol and other phenolic compounds are typically detected with techniques such as gas chromatography coupled to mass spectrometry[4,5] and/or solid-phase microextraction,[6,7] various spectroscopic techniques (surface-enhanced Raman spectroscopy,[8] infrared spectroscopy,[9] colorimetry,[10] fluorimetry[11]), and electrochemical sensing approaches (piezoelectric,[12,13] capacitive,[14] chemiresistive,[15,16] amperometric,[17,18] voltammetric,[18,19] impedance[20]). Although these routes offer promising analytical opportunities, there remains a need to develop robust, inexpensive, and disposable detectors that can be deployed autonomously without the need for laborious sample pretreatment or specific experimental conditions, such as increased temperature in the case of chemiresistive sensing.

At present, most electrochemical gas sensors exploit conductometric/chemiresistive principles.[21−23] They are usually based on selected metal oxides, which enable favorable sensitivity but somewhat limited selectivity and encounter difficulties under humid conditions or in the presence of sulfur compounds and weak acids.[24−26] In addition, these sensors mostly operate at elevated temperatures (100−500 °C) and are thus severely limited in practical use.[25,26] Even the conductometric sensors designed particularly for operation at ambient temperatures suffer from decreased stability and sensitivity, particularly after exposure to moisture or prolonged operation time.[22,23] Other but comparatively less common schemes include amperometric or voltammetric gas sensors.[27,28] Several approaches have been demonstrated, such as the incorporation of polymeric membranes for the separation of a liquid electrochemical cell from the outer atmosphere,[27] the employment of selected ionic liquids as

Received: May 12, 2020
Accepted: June 29, 2020
Published: June 29, 2020

https://dx.doi.org/10.1021/acssensors.0c00973
ACS Sens. 2020, 5, 2570−2577

nonvolatile electrolytes on the electrode surface,[17,29,30] and enzyme-based electrochemical sensors.[31,32]

Herein, we demonstrate a novel, simple voltammetric sensor based on sodium polyacrylate as an alkaline, semisolid, gel-like material enabling the accumulation of gaseous phenol, its deprotonation, and electrochemical oxidation into *p*-benzoquinone.[33] The sensor is functional under ambient conditions and susceptible to few interferences. It also shows sensitivity to other phenolic compounds, such as guaiacol and creosol, but at different electrode potentials, demonstrating favorable selectivity for phenolic compounds and possible differentiation among selected substances of this class.

EXPERIMENTAL SECTION

Materials and Reagents. Methanol (VWR International); ethanol (Carlo Erba Reagents); acetone and 2-nitrophenol (both from Honeywell Riedel-de Haën); ammonia, hydrochloric acid, formaldehyde, and glacial acetic acid (all from Merck); and benzaldehyde, phenol, creosol, guaiacol, and syringol (all from Sigma-Aldrich) were of the analytical grade. Pure O_2 was received from Messer. Test solutions yielding the desired gaseous-phase analyte concentrations according to Henry's law[34] were prepared in tightly closed 100 mL glass flasks. All solutions used in this work were prepared using Milli-Q water (R = 18.2 MΩ). A plastic artifact used to test the sensor's performance in a complex real sample was provided by the Institute for Sustainable Heritage, University College London, United Kingdom.[3]

Synthesis and Characterization of the Sensing Material. Sodium polyacrylate was prepared by mixing 5.0 mL of a 1.0 M NaOH solution (Sigma-Aldrich) with 0.18 g of solid polyacrylic acid (450 000 g mol^{-1}; Sigma-Aldrich), which resulted in a NaOH/polyacrylic acid molar ratio of 2:1, sodium polyacrylate mass concentration of 7%, and a pH of 14. Ionic conductivity measurements (σ, S cm^{-1}) of the sodium polyacrylate were carried out by electrochemical impedance spectroscopy using an Autolab PGSTAT30 (Metrohm/Eco Chemie) equipped with a frequency response analyzer and platinum electrodes. Rheological studies were performed with a Physica MCR 301 rheometer using a cone-plate stainless steel sensing system CP50/2 at 25 °C and a zero gap of 0.209 mm (Anton Paar). Infrared spectra were recorded on a monocrystalline silicon wafer substrate using an IFS 66/S Fourier transform infrared (FTIR) spectrometer (Bruker Optics) in transmission mode over the range of 4000−650 cm^{-1} with a resolution of 4 cm^{-1}. One measurement consisted of an average of 128 spectra. Thermogravimetric analysis was conducted with a thermogravimetric analyzer (Mettler Toledo) equipped with the STARe Excellence software in a N_2 atmosphere (20 mL min^{-1}) in the range of 30−1000 °C with a temperature ramp of 10 °C min^{-1}.

Electrochemical Measurements. The measurements were conducted immediately after drop-casting 20 μL of sodium polyacrylate onto a screen-printed electrode (DRP-110, Metrohm DropSens, designed for working with microvolumes), which consists of a carbon working electrode (d = 4 mm), a carbon counter electrode, and a silver quasi-reference electrode (Figure 1). Cyclic voltammetric and square-wave voltammetric measurements in the gas phase were carried out using a portable PalmSens4 potentiostat/galvanostat (PalmSens BV) in combination with a cable connector for screen-printed electrodes (DRP-CAC 71606, Metrohm DropSens) and the PSTrace 5.7 software (PalmSens BV). All measurements were performed at room temperature (22−23 °C) in a model atmosphere above the corresponding analyte solutions and in the presence of atmospheric gases. The electrode topography was recorded with the Ametek Zygo ZeGage Pro HR 3D optical profiler system.

Gas Chromatography−Mass Spectrometry with Flame Ionization Detection (HS−GC−MS). The results of electrochemical detection were validated with an Agilent 7890B gas chromatograph. The system consisted of a 7697A headspace sampler, a 7890B inlet, and a 5977A single quadrupole MS detector. The data were acquired with the Agilent MassHunter software. The separations were performed on a Zebron ZB-5 ms analytical column (30 mm × 0.32 mm × 1.0 μm).

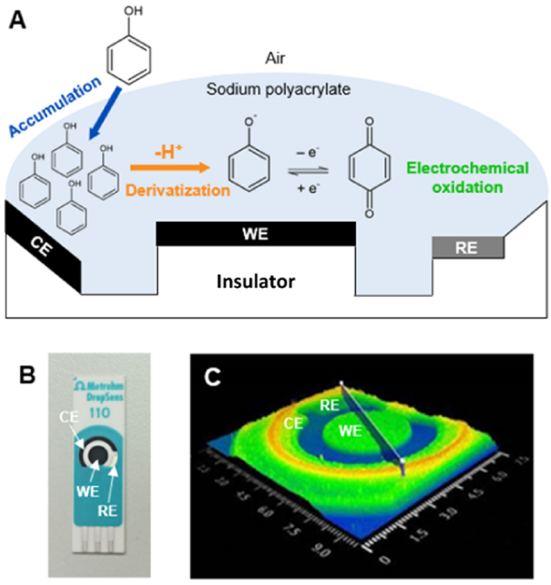

Figure 1. (A) Scheme of the detection principle. (B) Image of the supporting screen-printed electrode. (C) Topographical profile of the electrodes with a lagooned geometry for working with microvolumes. CE, counter electrode; WE, working electrode; RE, reference electrode.

The determination of phenol content in the vapor phase was performed with headspace GC−MS as follows. Headspace parameters: loop temperature, 185 °C; transfer line temperature, 190 °C; oven temperature, off (room temperature); equilibration time, 0 min; injection time, 1 min; cycle duration, 19 min; shaking, 136 times/min. GC parameters: injection temperature, 275 °C; split injection mode; split ratio, 1:1; helium mobile phase; pressure on the chromatographic column 4 psi (flow, 3.27 mL min^{-1}); column temperature gradient, 80 °C//10 °C min^{-1}//230 °C (0 min); transfer line temperature, 280 °C.

The MS detection was held on a single quadrupole detector in the SIM mode at m/z values of 39.00, 66.00, and 94.00. The chromatogram was scanned in a 2 min time segment with a solvent delay of 2 min. For all three SIM m/z values, the detector gain factor was set to 0.800, and the dwell time was set to 10.

RESULTS AND DISCUSSION

Sodium Polyacrylate Characterization. The infrared spectrum of sodium polyacrylate revealed the expected absence of carboxylic protons, which had been exchanged with sodium cations. The −OH vibrations with a broad signal at 3367 cm^{-1}, low signal at 2200 cm^{-1}, and a shoulder at 856 cm^{-1} could be ascribed to a weak hydrogen bond, showing the existence of residual water (Figure 2A). Accordingly, the thermogravimetric profile (Figure 2B) showed the presence of weakly bound water followed by polymer decomposition. Viscosity decreased almost exponentially from approximately 250 000 mPa·s at a shear rate of 1 rpm to 20 000 mPa·s at 100 rpm (Figure 2C), which is a typical behavior of entangled long polymer chain molecules becoming untangled/ordered with increasing shear rate (shear thinning). The shear stress increased nonlinearly with increasing shear rate and leveled off at approximately 50 rpm, reflecting possible structure degradation above this value (Figure 2D).

https://dx.doi.org/10.1021/acssensors.0c00973
ACS Sens. 2020, 5, 2570−2577

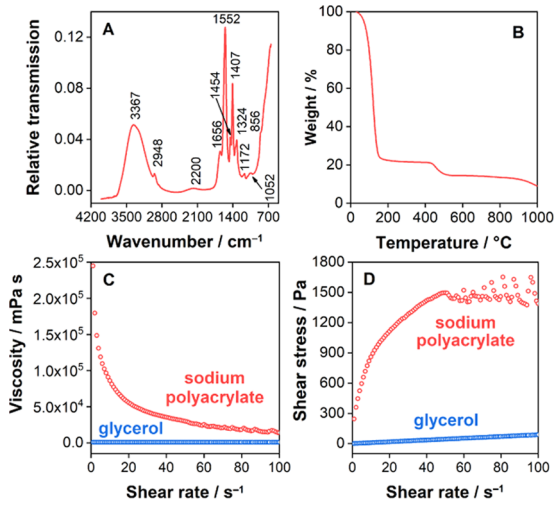

Figure 2. Physicochemical and rheological properties of sodium polyacrylate. (A) Infrared transmission spectrum. (B) Thermogravimetric profile in an N_2 atmosphere at 10 °C min^{-1}. (C) Viscosity and (D) shear stress after 8 h aging in N_2 flow (red) in comparison to glycerol as a typical model Newtonian liquid (blue).

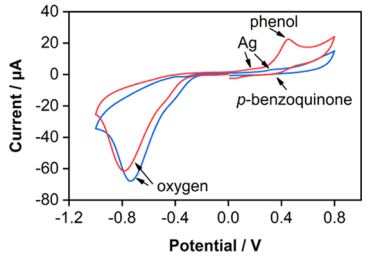

Figure 3. Cyclic voltammograms of 1.0 ppmv gaseous phenol after 30 min accumulation (red) together with a background response (blue) obtained at the sodium-polyacrylate-based gas sensor. The scan rate was 100 mV s^{-1}.

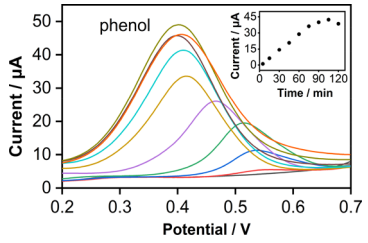

Figure 4. Square-wave voltammograms for nine successive measurements of 1.0 ppmv phenol in 15 min accumulation intervals (color lines) together with the background response (gray line). All measurements were taken with the same sensor. Square-wave voltammetric scan with a frequency of 25 Hz, an amplitude of 50 mV, and a potential step of 4 mV. The inset shows the corresponding calibration plot.

As anticipated due to the presence of Na^+ and OH^-, the ionic conductivity measurement yielded a relatively high value of 26.4 mS cm^{-1}, which is in accordance with good electrochemical operation. We can conclude that sodium polyacrylate displays a semisolid consistency together with strong intermolecular interactions due to long polymer chains, as well as possible intermolecular cross-linking/coordination with sodium cations. Thus, it exhibits a non-Newtonian (pseudo-plastic) character, compared to a typical model Newtonian liquid, such as glycerol.

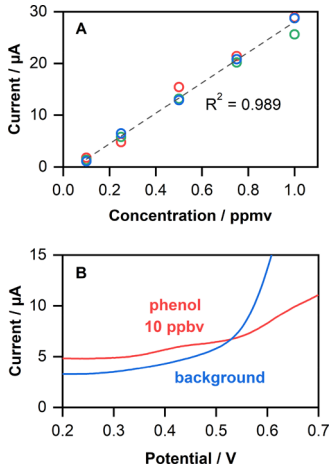

Figure 5. (A) Signal height plot for increasing concentrations of gaseous phenol in the range of 0.1−1.0 ppm after 60 min accumulation (three different sensors per time point). (B) Square-wave voltammograms in the presence of only 10.0 ppbv gaseous phenol after 120 min accumulation (red) together with the background (blue). Other conditions are as in Figure 3.

Table 1. Effect of Selected Potentially Interfering Organic and Inorganic Compounds on the Oxidation Potential of 1 ppmv of Phenol after 30 min Accumulation[a]

	concentration		
compound	100 ppbv	1 ppmv	10 ppmv
methanol	no effect (n = 2)	no effect (n = 2)	potential shift of ±25 mV (n = 3)
ethanol	no effect (n = 2)	no effect (n = 2)	no effect (n = 2)
formaldehyde	anodic shift for ca. 40 mV (n = 3)	anodic shift for ca. 50 mV (n = 3)	anodic shift for ca. 230 mV (n = 3)
benzaldehyde	no effect (n = 2)	no effect (n = 2)	no effect (n = 2)
acetone	no effect (n = 2)	no effect (n = 2)	no effect (n = 2)
acetic acid	no effect (n = 2)	no effect (n = 2)	no effect (n = 2)
HCl	no effect (n = 2)	no effect (n = 2)	no effect (n = 2)
NH_3	no effect (n = 2)	no effect (n = 2)	no effect (n = 2)

[a]Two or three measurements with different sensors were taken per concentration of an individual interferent. Other conditions are as in Figure 3.

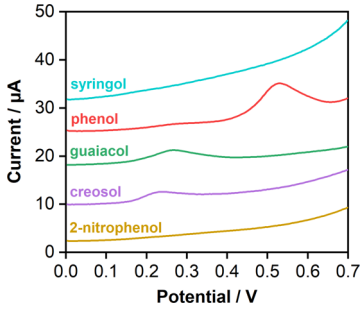

Figure 6. Square-wave voltammograms in the presence of 0.5 ppmv gaseous syringol (turquoise), phenol (red), guaiacol (green), creosol (violet), and 2-nitrophenol (ocher) after 30 min accumulation. Other conditions are as in Figure 3.

Electrochemical Characterization. Preliminary cyclic voltammetric experiments under ambient conditions in the

https://dx.doi.org/10.1021/acssensors.0c00973
ACS Sens. 2020, 5, 2570−2577

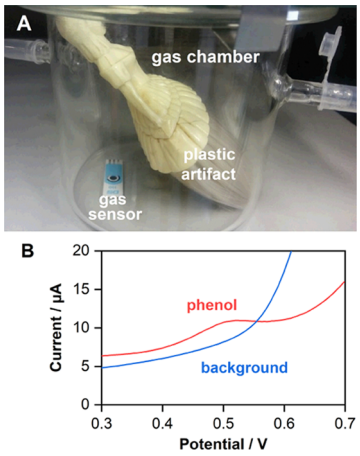

Figure 7. (A) Photo of the plastic artifact in a glass chamber together with an exposed gas sensor. (B) Square-wave voltammogram of gaseous phenol released from the artifact after 30 min (red) together with the background response (blue). Other conditions are as in Figure 3.

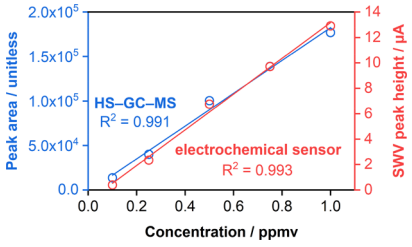

Figure 8. Calibration curves obtained with the novel electrochemical gas sensor after 30 min accumulation (red) and HS−GC−MS (blue) for the same phenol standards. Each calibration point is an average of three individual measurements (three different sensors in the case of electrochemical detection). Other conditions pertaining to the sensor are as in Figure 3.

potential range of −1.0 to +0.8 V revealed a phenol oxidation signal at approximately +0.5 V (Figure 3). The alkaline environment of sodium polyacrylate (pH = 14) promoted the accumulation and electrochemical oxidation of gaseous phenol to *p*-benzoquinone through the phenolate intermediate.[33] Accordingly, a weak *p*-benzoquinone reduction peak could be observed at approximately +0.4 V (Figure 3). Sodium polyacrylate mixtures with different molar ratios of NaOH and polyacrylic acid (2:1, 1:1, and 1:2) and pure polyacrylic acid were also tested; the mixture of NaOH/polyacrylic acid = 2:1 exhibited the highest response to gaseous phenol (data not shown) and was thus selected for further studies.

In the cathodic region, the sensor showed a strong signal at ca. −0.8 V due to the oxygen reduction reaction (Figure 3), which was corroborated by purging the experimental atmosphere with pure O_2. However, since the presence of O_2 did not interfere with the phenol signal in the anodic region, this process was not further investigated. A weak oxidation signal was also observed at around +0.2 V, presumably due to silver leaching from the quasi-reference silver electrode; this signal was present in all measurements and did not interfere with the phenol signal. All of the following studies were done in the square-wave voltammetric mode in the range of 0.0 to +0.7 V.

The sensor maintained a stable electroanalytical performance for approximately 30 min of exposure to ambient air, after which it began to dry and lose its sensitivity to gaseous analytes. However, a dried sensor (e.g., after being exposed to ambient air overnight) could be recovered by exposing it to a humid atmosphere, e.g., above the water surface in a water-filled flask. Still, the response to gaseous analytes remained attenuated. For example, the response of such a recovered sensor after a 30 min exposure to 1.0 ppmv of phenol was about 36% of the response of a freshly prepared sensor (data not shown). Thus, all of the following measurements were done with freshly prepared sensors.

Electroanalytical Performance Study. The influence of the accumulation time upon the sensor's voltammetric response was studied at a phenol concentration of 1.0 ppmv (Figure 4), which is at the low end of the typical detection range of chemiresistive sensors.[23] The response initially increased almost linearly with increasing accumulation time and started to level off at 105 min, implying the saturation of the sensing surface. Therefore, the accumulation time of 60 min was selected as optimal under these conditions. In addition, when increasing the accumulation time, a shift of the phenol signal toward less positive potentials could be observed; this phenomenon can be attributed to lower reaction reversibility and different analyte diffusion pattern at this sensor setup.[35]

The sensor's response to gaseous phenol was linear in the examined concentration range of 0.1−1.0 ppmv after 60 min accumulation (Figure 5A, showing three different sensors per time point, R^2 = 0.989). Notably, a very high sensor-to-sensor reproducibility was achieved; the intersensor relative standard deviation was 6.8% after a 15 min accumulation of 500 ppbv phenol (n = 10). The proposed sensor was also tested for trace phenol concentrations and found to yield a detectable and measurable signal after a 120 min accumulation of only 10.0 ppbv phenol (Figure 5B). Even lower detection limits could be anticipated at longer accumulation times.

It is important to note that transferring the sensor from phenol-containing (500 ppbv) to phenol-free atmosphere for 30 min did not result in signal attenuation. Moreover, after the second exposure to 500 ppbv of phenol for 30 min, the accumulation continued, and the signal became superimposed on the previous one, resembling the signal after uninterrupted exposure to 500 ppbv of phenol for 60 min. Continuous cycling voltammetry in the phenol-free atmosphere in the potential range of 0.0 to +0.8 V attenuated the phenol peak with each cycle, but only for approximately 79% after 20 cycles (data not shown). It can be assumed that under these conditions, a relatively stable redox system was established when gaseous phenol was accumulated in alkaline sodium polyacrylate medium, and continuous cycling only depleted the diffusion layer but not the bulk electrolyte.

Interferences. The sensor's operation was investigated in the presence of selected organic and inorganic gaseous compounds. No response to up to 500 ppmv of methanol, ethanol, formaldehyde, benzaldehyde, acetone, acetic acid, ammonia, or hydrochloric acid was detected by cyclic voltammetry in the examined potential window of −1.0 to +0.8 V after 30 min accumulation (data not shown). In the next step, the sensor was exposed to a mixture of 1 ppmv of phenol and 100 ppbv, 1 ppmv, or 10 ppmv of each of the listed gaseous compounds (Table 1). Again, none of the listed compounds at any of the tested concentrations affected the phenol signal height. However, formaldehyde caused the phenol signal to shift in the anodic direction, and 10 ppmv

https://dx.doi.org/10.1021/acssensors.0c00973
ACS Sens. 2020, 5, 2570−2577

Table 2. Phenol Detection Limits of Several Comparable Gas Sensors Based on Electrochemical Sensing Approaches[a]

type of sensor for gaseous phenol	lowest measured phenol concentration	advantages	disadvantages	reference
enzyme microbiosensor based on polyphenol oxidase (amperometric)	30 ppb	unhindered stability for 5 days	sensitive to temperature and relative humidity fouling of the electrode surface by quinone polymer formation	31
enzyme/gas-diffusion electrode based on tyrosinase (amperometric)	14 ppb[b] (above a 10 μM phenol solution)	remains active for more than 20 days sensitive to other phenolic compounds (*p*-cresol, 4-chlorophenol)	requires sufficient oxygen supply for the enzyme to operate	32
extracts of *Pleurotus ostreatus* mushroom (piezoelectric)	6.5 ppm	fast response (25−30 s) reversible	sensitive to relative humidity (operative at ≤60%)	12
an array of commercial gas sensors (Figaro, Inc.) based on polycrystalline SnO_2 (chemiresistive)	10 ppm	fast response (2−4 min) operative at room temperature enables sample fingerprinting	individual sensors are nonspecific complex data analysis is required (cluster analysis, principal component analysis)	15
filter paper soaked in ionic liquid (amperometric)	14 ppm[b] (above a 10 mM phenol solution)	fast response in flow injection analysis (base peak width <6 s) Inexpensive supporting material	selectivity and interferences not reported	17
filter paper soaked in ionic liquid (amperometric)	7 ppb[b] (above a 5 μM phenol solution)	fast response in flow injection analysis (base peak width <6 s) Inexpensive supporting material	selectivity and interferences not reported	30
reduced graphene oxide/metal oxide p−n heterojunction aerogel (chemiresistive)	10 ppb	operative at room temperature reversible and stable	several interferences (NH_3, O_2, ethanol, methanol, benzene, methylbenzene)	16
porous graphene oxide (capacitive)	75 ppm	operative at room temperature fast response and recovery reversible Selectivity can be achieved by graphene oxide functionalization	sensitive to relative humidity nonfunctionalized graphene oxide is prone to interferences (ammonia, ethanol, toluene, cyclohexane)	14
alkaline sodium polyacrylate/commercial screen-printed carbon electrodes (voltammetric)	≤10 ppb	straightforward, disposable setup few interferences operative at room temperature sensitive to other phenolic compounds, but selectively	prone to drying after prolonged exposures formaldehyde causes a signal shift irreversible	this work

[a]The study selection is not exhaustive. [b]Our recalculation based on Henry's constant for phenol.[34]

https://dx.doi.org/10.1021/acssensors.0c00973
ACS Sens. 2020, 5, 2570−2577

methanol caused the oxidation potential to shift for ±25 mV around the expected +0.5 V (Table 1). The anodic shift caused by formaldehyde could be explained through the emergence of base-catalyzed polymeric products of phenol and formaldehyde, which is a well-known reaction exploited in the production of phenol−formaldehyde resins. On the other hand, a signal shift due to the presence of methanol could be explained by enhanced drying of the sensor surface or the effect on the binder that holds the screen-printed system together.

Response to Other Phenolic Compounds. The sensor was further studied for the detection of 2-nitrophenol, a precursor in the manufacture of dyes, rubber, and fungicides; guaiacol (2-methoxyphenol), a component of wood smoke, essential oils, and flavors; syringol (2,6-methoxyphenol), another important component of wood smoke; and creosol (4-methyl-2-methoxyphenol), a disinfectant. The sensor did not respond to 0.5 ppmv of 2-nitrophenol or syringol in the potential range of 0.0 to +0.7 V, whereas the same concentration of guaiacol and creosol yielded a signal at ca. +0.26 and +0.23 V, respectively (Figure 6). It is evident that the peaks of guaiacol and creosol were well distinguished from the one of phenol and that every additional functional group decreased the sensitivity of the sensor for these compounds. Further studies are necessary to fully characterize the sensor's responsiveness and discriminatory power for various phenolic compounds.

Performance in a Complex Real Sample. The sensor's suitability for practical application was successfully demonstrated by exposing the sensor for 30 min to a real plastic artifact known to emit phenol[3] under ambient conditions (Figure 7A). As can be seen, the released phenol was accumulated and readily detected against the flat background recorded in the absence of the plastic artifact (Figure 7B). The concentration of emitted phenol was calculated to be 174 ppbv (taken with three different sensors). No peaks indicative of other phenolic compounds were observed.

Comparison to a Standard Analytical Method. The sensor's performance was compared to that of the HS−GC−MS technique. First, HS−GC−MS was used to check the sensor's response to the standard solutions used for its calibration. As can be seen in Figure 8, both calibration curves closely matched. Second, HS−GC−MS was used to validate the determination of phenol emissions from the plastic artifact. Since the HS−GC−MS headspace needs to be heated above room temperature to function properly, this changes the experimental conditions, and the obtained values are not directly comparable to those yielded by the electrochemical sensor for the same sample headspaces. Therefore, the results should be appropriately corrected for the change in Henry's constant with temperature.[36] The concentration obtained by the HS−GC−MS and corrected for Henry's constant was 115 ppbv, which matches well with the result of the electrochemical sensor. One should also consider that the plastic artifact does not necessarily emit phenol at a constant rate. Furthermore, in line with the electrochemical sensor, no additional molecular fragments indicative of other phenolic compounds were detected with HS−GC−MS.

Comparison with Similar Phenol Sensors. Although the literature on sensors for phenol dissolved in aqueous and nonaqueous media is abundant, there are comparatively much fewer reports on sensors for gaseous phenol. Some typical examples are collected in Table 2. As can be seen, amperometric and voltammetric sensors are generally able to reach lower detection limits and are more selective to phenol and other phenolic compounds than piezoelectric, capacitive, or chemiresistive sensors. A notable exception is the chemiresistive sensor based on reduced graphene oxide/metal oxide p−n heterojunction aerogel, which was reported to detect 10 ppb phenol under ambient conditions yet still suffered from considerable cross-reactivity to ammonia, oxygen, ethanol, methanol, benzene, and methylbenzene.[16] In comparison to the listed sensors, the sensor described in this work is undoubtedly competitive and offers an additional benefit of a simple sensory material synthesis and facile sensor preparation (i.e., a simple drop-casting from the preprepared sensing solution), which does not require specialist knowledge. The sensor's disadvantages, particularly the tendency of the sensory material to dry with time, will be addressed in our future research using ionic liquids. However, as demonstrated in this work, the use of freshly prepared disposable sensors is completely feasible.

CONCLUSIONS

Alkaline sodium polyacrylate drop-cast onto a commercial screen-printed carbon electrode was demonstrated to yield a highly sensitive disposable sensor for the detection of gaseous phenol. The sensor's sensitivity to some other phenolic compounds at the potentials that are well differentiated from that of phenol, in combination with the insensitivity to several potentially interfering organic and inorganic gases, gives room for further optimization of its selectivity and multianalyte sensing. The presented sensor thus provides a solid foundation for the future development of sensitive and robust gas sensing systems that could be applicable in the fields of environmental monitoring, preservation of cultural heritage, and reduction of occupational health hazards.

AUTHOR INFORMATION

Corresponding Author

Samo B. Hočevar − *Department of Analytical Chemistry, National Institute of Chemistry, SI-1000 Ljubljana, Slovenia;* orcid.org/0000-0003-2980-4822; Phone: +386 1 4760 230; Email: samo.hocevar@ki.si

Authors

Tea Romih − *Department of Analytical Chemistry, National Institute of Chemistry, SI-1000 Ljubljana, Slovenia;* orcid.org/0000-0003-2092-4844

Eva Menart − *Department of Analytical Chemistry, National Institute of Chemistry, SI-1000 Ljubljana, Slovenia*

Vasko Jovanovski − *Department of Materials Chemistry, National Institute of Chemistry, SI-1000 Ljubljana, Slovenia*

Andrej Jerič − *Center for Validation Technologies and Analytics, National Institute of Chemistry, SI-1000 Ljubljana, Slovenia*

Samo Andrenšek − *Center for Validation Technologies and Analytics, National Institute of Chemistry, SI-1000 Ljubljana, Slovenia*

Complete contact information is available at: https://pubs.acs.org/10.1021/acssensors.0c00973

Author Contributions

Author contributions are defined according to the CRediT contributorship model. T.R. contributed to investigation, formal analysis, and writing original draft. E.M. was involved in conceptualization, methodology, and investigation. V.J. was

https://dx.doi.org/10.1021/acssensors.0c00973
ACS Sens. 2020, 5, 2570−2577

involved in conceptualization and resources. A.J. performed investigation and formal analysis. S.A. contributed to methodology, supervision, and writing original draft. S.B.H. was involved in funding acquisition, supervision, writing, and review & editing.

Funding

This research received funding from the European Union's Horizon 2020 NanoRestArt project (grant agreement no. 646063) and the Slovenian Research Agency (P1-0034).

Notes

The authors declare no competing financial interest.

■ ACKNOWLEDGMENTS

The authors thank Helena Spreizer and Matic Šobak from the Department of Materials Chemistry for technical assistance.

■ REFERENCES

(1) European Chemicals Agency Home Page. Substance Information: Phenol. https://echa.europa.eu/substance-information/-/substanceinfo/100.003.303 (accessed Dec 4, 2019).
(2) United States Environmental Protection Agency Home Page. Initial List of Hazardous Air Pollutants with Modifications. https://www.epa.gov/haps/initial-list-hazardous-air-pollutants-modifications (accessed Dec 4, 2019).
(3) Curran, K.; Underhill, M.; Gibson, L. T.; Strlic, M. The development of a SPME-GC/MS method for the analysis of VOC emissions from historic plastic and rubber materials. *Microchem. J.* **2016**, *124*, 909−918.
(4) Bajoub, A.; Pacchiarotta, T.; Hurtado-Fernández, E.; Olmo-García, L.; García-Villalba, R.; Fernández-Gutiérrez, A.; Mayboroda, O. A.; Carrasco-Pancorbo, A. Comparing two metabolic profiling approaches (liquid chromatography and gas chromatography coupled to mass spectrometry) for extra-virgin olive oil phenolic compounds analysis: A botanical classification perspective. *J. Chromatogr. A* **2016**, *1428*, 267−279.
(5) Boczkaj, G.; Makoś, P.; Przyjazny, A. Application of dynamic headspace and gas chromatography coupled to mass spectrometry (DHS-HS−GC−MS) for the determination of oxygenated volatile organic compounds in refinery effluents. *Anal. Methods* **2016**, *8*, 3570−3577.
(6) Jain, A.; Soni, S.; Reddy-Noone, K.; Pillai, A. K. K. V..; Verma, K. K. Combined headspace single-drop microextraction and solid-phase microextraction for the determination of phenols as their methyl ethers by gas chromatography-mass spectrometry. *Anal. Methods* **2017**, *9*, 6590−6598.
(7) Liu, L.; Meng, W.-K.; Li, L.; Xu, G.-J.; Wang, X.; Chen, L.-Z.; Wang, M.-L.; Lin, M.-J.; Zhao, R.-S. Facile room-temperature synthesis of a spherical mesoporous covalent organic framework for ultrasensitive solid-phase microextraction of phenols prior to gas chromatography-tandem mass spectrometry. *Chem. Eng. J.* **2019**, *369*, 920−927.
(8) Aguilar-Hernández, I.; Afseth, N. K.; López-Luke, T.; Contreras-Torres, F. F.; Wold, J. P.; Ornelas-Soto, N. Surface enhanced Raman spectroscopy of phenolic antioxidants: A systematic evaluation of ferulic acid, *p*-coumaric acid, caffeic acid and sinapic acid. *Vib. Spectrosc.* **2017**, *89*, 113−122.
(9) Wu, Z.; Xu, E.; Long, J.; Pan, X.; Xu, X.; Jin, Z.; Jiao, A. Comparison between ATR-IR, Raman, concatenated ATR-IR and Raman spectroscopy for the determination of total antioxidant capacity and total phenolic content of Chinese rice wine. *Food Chem.* **2016**, *194*, 671−679.
(10) Zhang, L.-p.; Xing, Y.-p.; Liu, L.-h.; Zhou, X.-h.; Shi, H.-c. Fenton reaction-triggered colorimetric detection of phenols in water samples using unmodified gold nanoparticles. *Sens. Actuators, B* **2016**, *225*, 593−599.
(11) Kose, M.; Kırpık, H.; Kose, A. Fluorimetric detections of nitroaromatic explosives by polyaromatic imine conjugates. *J. Mol. Struct.* **2019**, *1185*, 369−378.
(12) Silina, Y. E.; Kuchmenko, T. A.; Korenman, Y. I.; Tsivileva, O. M.; Nikitina, V. E. Use of a complete factorial experiment for designing a gas sensor based on extracts of *Pleurotus ostreatus* mycelium mushroom. *J. Anal. Chem.* **2005**, *60*, 678−683.
(13) Pan, M.; Li, R.; Xu, L.; Yang, J.; Cui, X.; Wang, S. Reproducible molecularly imprinted piezoelectric sensor for accurate and sensitive detection of ractopamine in swine and feed products. *Sensors* **2018**, *18*, No. 1870.
(14) Teradal, N. L.; Marx, S.; Morag, A.; Jelinek, R. Porous graphene oxide chemi-capacitor vapor sensor array. *J. Mater. Chem. C* **2017**, *5*, 1128−1135.
(15) Diz, V.; Cassanello, M.; Negri, R. M. Detection and discrimination of phenol and primary alcohols in water using electronic noses. *Environ. Sci. Tehnol.* **2006**, *40*, 6058−6063.
(16) Guo, D.; Cai, P.; Sun, J.; He, W.; Wu, X.; Zhang, T.; Wang, X.; Zhang, X. Reduced-graphene-oxide/metal-oxide p-n heterojunction aerogels as efficient 3D sensing frameworks for phenol detection. *Carbon* **2016**, *99*, 571−578.
(17) Dossi, N.; Toniolo, R.; Pizzariello, A.; Carrilho, E.; Piccin, E.; Battiston, S.; Bontempelli, G. An electrochemical gas sensor based on paper supported room temperature ionic liquids. *Lab Chip* **2012**, *12*, 153−158.
(18) Rocha, D. P.; Dornellas, R. M.; Cardoso, R. M.; Narciso, L. C. D.; Silva, M. N. T.; Nossol, E.; Richter, E. M.; Munoz, R. A. A. Chemically versus electrochemically reduced graphene oxide: improved amperometric and voltammetric sensors of phenolic compounds on higher roughness surfaces. *Sens. Actuators, B Chem.* **2018**, *254*, 701−708.
(19) Goulart, L. A.; Gonçalves, R.; Correa, A. A.; Pereira, E. C.; Mascaro, L. H. Synergic effect of silver nanoparticles and carbon nanotubes on the simultaneous voltammetric determination of hydroquinone, catechol, bisphenol A and phenol. *Microchim. Acta* **2018**, *185*, No. 12.
(20) Seo, H.-K.; Ameen, S.; Akhtar, M. S.; Shin, H. S. Structural, morphological and sensing properties of layered polyaniline nanosheets towards hazardous phenol chemical. *Talanta* **2013**, *104*, 219−227.
(21) Gliszczyńska-Świgło, A.; Chmielewski, J. Electronic nose as a tool for monitoring the authenticity of food. A review. *Food Anal. Methods* **2017**, *10*, 1800−1816.
(22) Spinelle, L.; Gerboles, M.; Kok, G.; Persijn, S.; Sauerwald, T. Review of portable and low-cost sensors for the ambient air monitoring of benzene and other volatile organic compounds. *Sensors* **2017**, *17*, No. 1520.
(23) Li, Z.; Li, H.; Wu, Z.; Wang, M.; Luo, J.; Torun, H.; Hu, P. A.; Yang, C.; Grundmann, M.; Liu, X.; Fu, Y. Q. Advances in designs and mechanisms of semiconducting metal oxide nanostructures for high-precision gas sensors operated at room temperature. *Mater. Horiz.* **2019**, *6*, 470−506.
(24) Castro-Hurtado, I.; Mandayo, G. G.; Castaño, E. Conductometric formaldehyde gas sensors. A review: From conventional films to nanostructured materials. *Thin Solid Films* **2013**, *548*, 665−676.
(25) Giannoukos, S.; Brkić, B.; Taylor, S.; Marshall, A.; Verbeck, G. F. Chemical Sniffing Instrumentation for Security Applications. *Chem. Rev.* **2016**, *116*, 8146−8172.
(26) Kaushik, A.; Kumar, R.; Arya, S. K.; Nair, M.; Malhotra, B. D.; Bhansali, S. Organic−Inorganic Hybrid Nanocomposite-Based Gas Sensors for Environmental Monitoring. *Chem. Rev.* **2015**, *115*, 4571−4606.
(27) Baron, R.; Saffell, J. Amperometric gas sensors as a low cost emerging technology platform for air quality monitoring applications: A review. *ACS Sens.* **2017**, *2*, 1553−1566.
(28) Banerjee, R.; Tudu, B.; Bandyopadhyay, R.; Bhattacharyya, N. A review on combined odor and taste sensor systems. *J. Food Eng.* **2016**, *190*, 10−21.

(29) Gębicki, J.; Kloskowski, A.; Chrzanowski, W.; Stepnowski, P.; Namiesnik, J. Application of ionic liquids in amperometric gas sensors. *Crit. Rev. Anal. Chem.* **2016**, *46*, 122−138.
(30) Toniolo, R.; Dossi, N.; Pizzariello, A.; Casagrande, A.; Bontempelli, G. Electrochemical gas sensors based on paper-supported room-temperature ionic liquids for improved analysis of acid vapours. *Anal. Bioanal. Chem.* **2013**, *405*, 3571−3577.
(31) Dennison, M. J.; Hall, J. M.; Turner, A. P. Gas-phase microbiosensor for monitoring phenol vapor at ppb levels. *Anal. Chem.* **1995**, *67*, 3922−3927.
(32) Kaisheva, A.; Iliev, I.; Christov, S.; Kazareva, R. Electrochemical gas biosensor for phenol. *Sens. Actuators, B Chem.* **1997**, *44*, 571−577.
(33) Uliana, M. P.; Vieira, Y. W.; Donatoni, M. C.; Corrêa, A. G.; Brocksom, U.; Brocksom, T. J. Oxidation of mono-phenols to para-benzoquinones: a comparative study. *J. Braz. Chem. Soc.* **2008**, *19*, 1484−1489.
(34) Sander, R. Compilation of Henry's law constants (version 4.0) for water as solvent. *Atmos. Chem. Phys.* **2015**, *15*, 4399−4981.
(35) Mirceski, V.; Skrzypek, S.; Stojanov, L. Square-wave voltammetry. *ChemTexts* **2018**, *4*, No. 17.
(36) Dohnal, V.; Fenclová, D. Air-Water Partitioning and Aqueous Solubility of Phenols. *J. Chem. Eng. Data* **1995**, *40*, 478−483.

https://dx.doi.org/10.1021/acssensors.0c00973
ACS Sens. 2020, 5, 2570−2577